Road surface *n*-factors across elevational and latitudinal treelines, Dempster–ITH corridor, western Arctic Canada

Emma J. Stockton[1], Christopher R. Burn[1], M. Alice Wilson[2] & Steven V. Kokelj[2]
[1]*Carleton University, Ottawa, Ontario, Canada*
[2]*Northwest Territories Geological Survey, Government of Northwest Territories, Yellowknife, Northwest Territories, Canada*

Abstract

Relationships between air and ground surface temperatures can be summarized by *n*-factors for the freezing (n_f) and thawing (n_t) seasons. The theory of *n*-factors assumes that a homogenous surface, such as a road, has spatially consistent relationships between ground surface and air temperatures. The 400 km Dempster–ITH corridor in NWT crosses elevational and latitudinal treelines between the territorial border and the Beaufort Sea coast. Road surface *n*-factors along the corridor have been determined at nine sites to examine their variation in the range of climatic environments encountered. They have also been compared with values from four borrow pits to examine the influence of snow on the *n*-factor. During the study, air temperatures varied from -42.6 to 26.2 °C over two years beginning in October 2020. Values for n_t varied from 1.00 to 1.36, while n_f varied from 0.89 to 1.06 at the road sites and 0.10 to 0.76 at the pits. Values for n_t of 1.26 and n_f of 0.96 appear robust for a gravel road across a range of climatic environments.

1 Introduction

Design and maintenance challenges imposed by frost action affect almost all of Canada's highway network. In permafrost regions, a common approach to highway design is to contain thaw penetration within the road embankment and protect underlying permafrost from thaw. Embankment and road surface integrity may be compromised if ice-rich permafrost beneath the embankment thaws and the driving surface settles (e.g., Alfaro et al. 2009). Engineers seldom have access to ground surface temperatures when designing road geometry. Such values are a product of the surface energy balance and require monitoring of several microclimatic variables if they are to be reliably determined. Instead, *n*-factors are used to estimate surface temperatures from projected air temperatures (Lunardini 1978). The indices were developed for constructed surfaces such as roads because the surface energy balance is simplified by the removal of ecological effects. The temperature indices from which *n*-factors are derived can be determined by the summation of mean daily temperatures in degree days (°C-d) for the freezing (FDD) and thawing (TDD) seasons (Thompson 1963). The freezing (n_f) and thawing (n_t) *n*-factors may be expressed as:

$$n_f = \frac{\mathrm{FDD_s}}{\mathrm{FDD_a}} \quad [1]$$

$$n_t = \frac{\mathrm{TDD_s}}{\mathrm{TDD_a}} \quad [2]$$

where the subscripts *s* and *a* denote the surface and air, respectively. The *n*-factor is dimensionless and ranges from 0 to ∞. Values near 1.0 indicate a close relation between air and surface temperatures; high n_f and n_t represent relatively cold winter and warm summer surfaces, respectively. Reliable determination of an *n*-factor requires concurrent measurements in the air and at the surface, which is often impractical. Engineers manage this issue by selecting rational values from published literature. The theory of *n*-factors assumes a homogenous surface, such as a road, should have spatially consistent thermal relationships with the atmosphere.

The applicability of *n*-factors for identical road surfaces may differ with location. For example, Instanes and Anisimov (2008) found that a value of 1.0 simulated measured ground temperatures well in Longyearbyen, Svalbard, but not in Fairbanks, AK, or Yakutsk, Russia. Using book values to determine the *n*-factor may lead to uncertainty in the frost depth of 25–30% (Johnston 1981). Differences may be associated with changes in net radiation, turbulent heat transfer, construction materials, and surface roughness (e.g., Lunardini 1978). To the authors' knowledge, no previous studies have attempted to quantify the spatial variability of *n*-factors along a highway transect through varying climatic zones.

The Dempster and Inuvik–Tuktoyaktuk Highways (the Dempster–ITH corridor) provide an opportunity to investigate *n*-factors across elevational and latitudinal treelines along gravel roads (Palmer et al. 2012; O'Neill et al. 2015). Values were also derived for gravel surfaces with snow accumulation in borrow pits to examine the influence of snow on the *n*-factor and duration of the freezing and thawing seasons in the same region.

2 Study Area

The Dempster–ITH corridor in Northwest Territories (NWT) traverses the traditional territories of the Inuvialuit, Nihtat Gwich'in, Gwichya Gwich'in, Tetlit Gwich'in, Vuntut Gwich'in, and Na-Cho Nyak Dun. This study focuses on the 400 km between the Yukon/NWT border and Tuktoyaktuk (Figure 1). The route is the only surface link from southern

https://doi.org/10.52381/ICOP2024.143.1

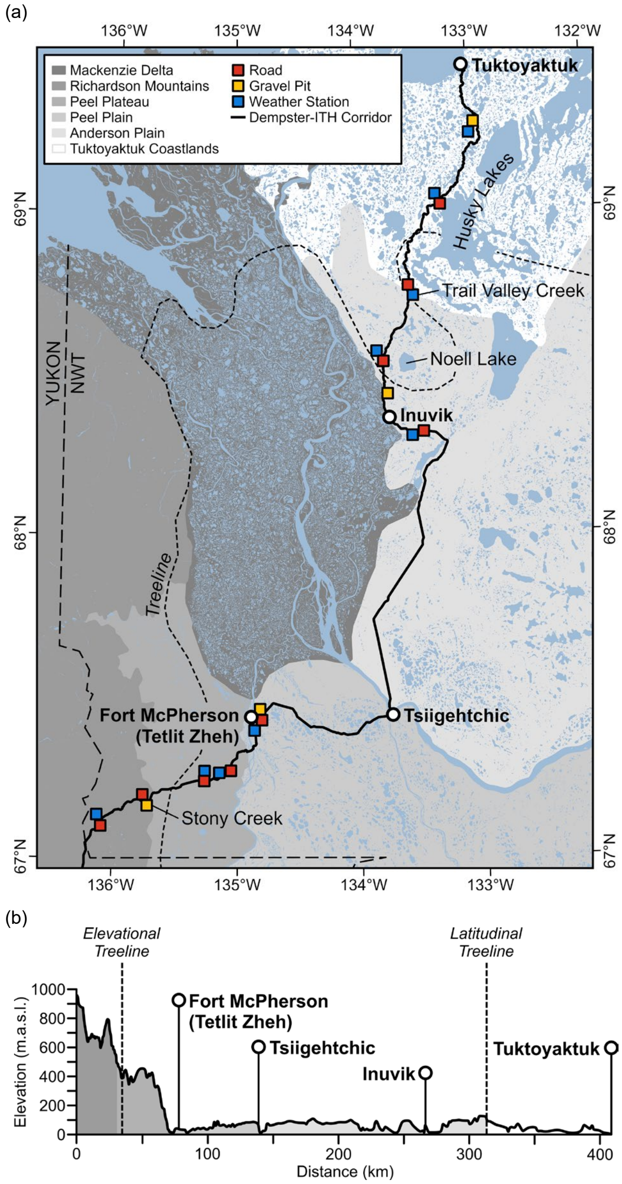

Figure 1. (a) Map with physiographic units and air and ground temperature monitoring sites across elevational treeline between the territorial border and Fort McPherson, and latitudinal treeline between Inuvik and Tuktoyaktuk (e.g., Ensom et al. 2020). (b) Elevation profile of the route with latitudinal treeline near Trail Valley Creek. Water bodies are from Canvec (Natural Resources Canada 2023).

Canada providing all-weather access for freight transport, private travel, tourism, and subsistence harvesting to Fort McPherson (Tetlit Zheh), Tsiigehtchic, Inuvik, and Tuktoyaktuk.

2.1 Highway Design and Construction

The Dempster Highway was completed in 1979 to a recommended embankment height of 1.4 m based on experience at Inuvik Airport (Johnston 1982). Post-construction surveys commended the serviceability of the highway but deemed the fill thickness insufficient in areas of flat, poorly drained terrain (Lingnau 1985). The conceptual design was a basal pad of sandstone and shale built directly on the ground and topped with a gravel driving surface. Suitable gravel sources were limited, so quarried limestone was also used as surfacing material (Huculak et al. 1978). The design of the ITH considered foreseeable changes in climate and permafrost conditions, the thermal influence of the embankment, and the sustainability of construction materials to meet the 75-year service life. Approximately 4.8 million m^3 of granular material were used to construct the ITH (Grozic and Zhang 2018). Embankment construction and borrow source extraction occurred in winter to minimize disturbance to the thaw sensitive terrain. The design incorporated an overbuild of about 0.45 m on top of the minimum thickness of 1.7–2.0 m, to account for settlement of frozen-placed materials in the summers following construction (Grozic and Zhang 2018). However, budget constraints reduced the fill in some areas and in turn the preservation of near-surface permafrost within a few years of the highway opening in 2017 (de Guzman et al. 2021).

2.2 Physiography, Climate, and Ground Temperatures

The corridor traverses several physiographic units and climatic regimes (Figure 1). At the territorial border, the climate is influenced by the elevation and topography of Richardson Mountains. Total annual precipitation is moderate (300–400 mm) and mostly falls in summer. Clear skies and low temperatures are common in January due to stabilized weather patterns from high-pressure cells (Wahl et al. 1987). Occasional disturbances in the shoulder seasons lead to higher temperatures and snowfall. The eastern flanks of the mountains mark the terminal limit of the Laurentide Ice Sheet.

Peel Plateau is a fluvially incised, glacially altered, and eastward sloping landscape. Permafrost is ice-rich and prone to thermokarst processes (Kokelj et al. 2017). FDD decreases with elevation due to strong atmospheric inversions resulting in mean winter temperatures on Peel Plateau about 4 °C higher than at Fort McPherson (O'Neill et al. 2015). Peel Plain is underlain by an ice-rich, fine grained till veneer over unexposed shale and mudstone bedrock quarried for the highway (Norris 1984). Mean annual air temperatures and total annual precipitation decrease northward from Fort McPherson (-7.3 °C, 300 mm) to Tuktoyaktuk (-10.1 °C, 160 mm; Environment Canada 2023).

North of Tsiigehtchic the corridor traverses Anderson Plain, an undulating and imperfectly drained landscape of gentle slopes, incised valleys, and uplands (Mackay 1963). Tuktoyaktuk Coastlands are characterised by thicker surficial deposits, few bedrock outcrops, and low, rolling terrain interspersed with lakes (Rampton 1988). Polygonal terrain is abundant and increases with proximity to the coast (Kokelj et al. 2014). TDD decreases northward due to onshore winds blowing across persistent sea ice and cold coastal waters, resulting in a mean monthly temperature difference of about 4 °C between Inuvik and Tuktoyaktuk in early summer (Burn 1997; Burn and Kokelj 2009).

The corridor is underlain by continuous permafrost but mean annual ground temperatures vary due to differences in climatic and environmental conditions. Across latitudinal treeline, permafrost temperatures decrease from about -3 °C in the forest to -6 °C in the tundra due to declining air temperatures and snow depth (Burn and Kokelj 2009). However, across elevational treeline, tundra permafrost is about 1 °C warmer than permafrost at Fort McPherson (-2.5 °C), due to higher winter air temperatures and earlier snow accumulation (O'Neill et al. 2015).

2.3 Treeline

Winter temperature inversions control a steep elevational gradient and treeline on Peel Plateau (O'Neill et al. 2015). The corridor descends from low shrub tundra in the mountains (≥ 1000 m asl), to tall shrub tundra (~400 m asl), to open canopies of black spruce (*Picea mariana*) and tamarack (*Larix laricina*) at Fort McPherson (~30 m asl). Latitudinal treeline crosses Anderson Plain north of Inuvik. It is associated with declining summer air temperatures due to differences in net radiation and onshore winds (Burn 1997). Anderson Plain is characterised by a sparse overstory of tamarack, black spruce, white spruce (*Picea glauca*), and paper birch (*Betula papyrifera*; Ritchie 1977). Tall shrub tundra prevails about 30 km north of Inuvik, while low shrub tundra occupies the polygonal terrain of the Tuktoyaktuk Coastlands. Alder (*Alnus spp.*) and willow (*Salix spp.*) are common in disturbed areas.

3 Methodology

In October 2020, nine road sites were established in the corridor to capture a range of thermal conditions at the highway surface across elevational and latitudinal treeline (Figure 1). Road surface temperatures were measured hourly using Geoprecision PT 1000 thermistors and M-Log5W data loggers. The instruments, housed in sealed PVC pipe, were installed by hand drill to a depth of 0.15 m below the highway centerline and the boreholes were backfilled with drill cuttings. The thermistor depth was recommended by Government of the Northwest Territories Department of Infrastructure (GNWT-INF) to prevent damage from maintenance operations, such as grading and snow ploughing. Thermistors were downloaded wirelessly to a laptop using FG2-Shell Geoprecision software.

Similar thermistors were installed at "gravel pits" where snow accumulated in winter. These include a gravel pad at Stony Creek and three borrow sources at Fort McPherson (FM500), Noell Lake (Pit I401A), and Husky Lakes (Pit 177). Thermistor cables with sensors up to 10 m depth were also installed at the two pits along the ITH and, at some locations beneath the road embankment (e.g., Rudy et al. 2020a,b). Data from 2–4 m depth at the Noell Lake pit (I401A) and road sites are used in the analysis. These boreholes were drilled by auger in 2017 and instrumented with Geoprecision PT 1000 and Lakewood RX-16 thermistors at the pit and road, respectively (Ensom et al. 2020).

Air temperatures were collected from nine weather stations along the route managed by Environment Canada and GNWT (Kokelj et al. 2022). Air and surface temperatures were divided into two years from 16th October 2020. Daily *n*-factors were calculated using eq. 1 and 2 and averaged seasonally, i.e., when both variables were < 0 °C for n_f or > 0 °C for n_t, since daily fluctuations may not be simultaneous.

Snow depth and density were measured at the gravel pits in late March to mid April. Median snow depth was calculated from five measurements with a metal meter stick. Snow density was measured using a Metric Prairie Snow Sampler (Geo Scientific Ltd., Vancouver, BC) with Lexan graduated plastic tube and steel cutter. Samples were placed in a clear plastic bag and weighed using a Pesola Medio Spring Scale. The density was calculated from the snow mass and volume occupied in the tube.

4 Defining the Freezing and Thawing Seasons

For this paper, the onset and duration of the freezing (S_f) and thawing seasons (S_t) were defined by daily *n*-factors and varied between sites. The seasons began when the *n*-factor was calculable for three consecutive days, i.e., both air (T_a) and surface temperatures (T_s) were of the same sign. If a period of equal or greater length without a *n*-factor followed, the season would restart. The end of the seasons was delineated by the cessation of *n*-factors for three or more days. S_f and S_t were separated by spring and autumn when T_a and T_s fluctuated asynchronously. At the end of the season, T_a and T_s were close at the road sites. However, in the pits, T_s lagged T_a due to the intervening snowpack. When T_a was higher than T_s, but below 0 °C, the daily *n*-factor might be large. In this case, *n*-factors greater than three standard errors above the seasonal mean were neglected (i.e., $n_f \gtrsim 1.7$ and $n_t \gtrsim 2.7$).

At the road, S_f and S_t were long and well-defined because T_s conformed to changes in T_a. Installation of the road thermistors in mid October 2020 missed the start of S_f by one or two weeks. At the road, S_f began in late September to early October and ended in mid to late April, lasting 186–214 days. The length of S_f was similar among the sites each year, but it began earlier at higher elevations. S_t started in early June and ended in late September, lasting 104–115 days. During spring and autumn, T_a and T_s were close to 0 °C and had relatively little impact on seasonal FDD or TDD. The duration of spring was relatively consistent (45–51 days), while autumn was shorter at higher elevations (3 days) than north of Fort McPherson (14 days).

At the gravel pits, the onset and duration of the seasons were similar to the road, but T_s did not fluctuate to the same extent as at the road during S_f due to the snow cover. S_f started in early to mid October and ended in mid April to mid May, lasting 177–214 days. Each year the onset of S_f was similar among sites, but the season was extended by up to four weeks at Husky Lakes (Pit 177) due to continuously cool air temperatures near the coast. At the remaining pits, the duration of S_f was about ten days shorter than the road due to the air temperature being between 0 °C and T_s, as discussed above. S_t at the pits was comparable to the road with an onset in early June and a duration of 104–113 days. The duration of spring ranged from 19–53 days, while autumn lasted 14–22 days. Longer S_f at Husky Lakes (Pit 177) resulted in a shorter spring and rapid transition to summer.

5 AIR AND ROAD SURFACE TEMPERATURES

Figure 2 is a scatter plot of monthly mean temperatures for T_a and T_s at each site over two years. The measurements have equal precision; thus, the relation can be summarized using the functional fit, in this case the principal axis (Mark and Church 1977). The data show a strong, linear correlation with higher T_s than T_a over the year. Data with slightly increased scatter from -10 to 10 °C are the shoulder seasons. Figure 3 shows daily mean T_a and T_s at all sites with principal axes for S_f and S_t.

The principal axis in Figure 2 and the seasonal means in Table 1 indicate T_s was higher than T_a, except for the Territorial Border in 2020–2021. The principal axes in Figure 3 yield a summary of the relation on a daily, rather than a seasonal basis. For S_t, the functional relation indicates T_s is about 2.4 °C higher than T_a, which is comparable to data in Table 1. Data from spring and autumn are not included in Figure 3. In 2020–2021, the range in annual mean T_s was 2.5 °C among all nine sites, and 1.5 °C across both gradients (Table 1). During this period, the surface offset (T_s–T_a) was 1.7–1.8 °C across latitudinal treeline (Inuvik to Husky Lakes), and 1.1–2.6 °C across elevational treeline (Territorial Border to Fort McPherson). At higher elevations, T_s during S_t was lower than Fort McPherson, while T_s during S_f was higher due to atmospheric inversions.

6 THE *N*-FACTOR

6.1 Road Surface *n*-factors

The seasonal mean *n*-factors shown in Table 1 are within the large range of values reported in the literature for cleared gravel surfaces. Published n_f vary from 0.60–1.00 and n_t from 1.00–2.01 (e.g., Johnston 1982). Over the study period, n_f and n_t varied from 0.89–1.06 and 1.08–1.36, respectively (Table 1). Mean n_f and n_t for the entire corridor are 0.96 and 1.26, respectively. During S_t, surface temperatures are a result of available radiation and advected air mass characteristics, while during S_f air and surface temperatures are primarily a function of the prevailing air masses. Hence, n_t is generally higher than n_f.

Among sites, values for n_f and n_t evolve similarly over the season as degree day totals progressively increase. Figure 4 illustrates this with daily cumulative *n*-factors and daily cumulative degree days for the Noell Lake road site. At the beginning of the season *n*-factors fluctuate because degree day totals are low and sensitive to small changes in T_s or T_a. As the seasons advance, *n*-factors become insensitive to daily temperature changes due to the large degree day totals, causing oscillations to dampen and the ratio to level off. The *n*-factor is stable when daily cumulative values differ from the seasonal mean by less than 10%. Along the corridor daily cumulative *n*-factors stabilized after one to three weeks.

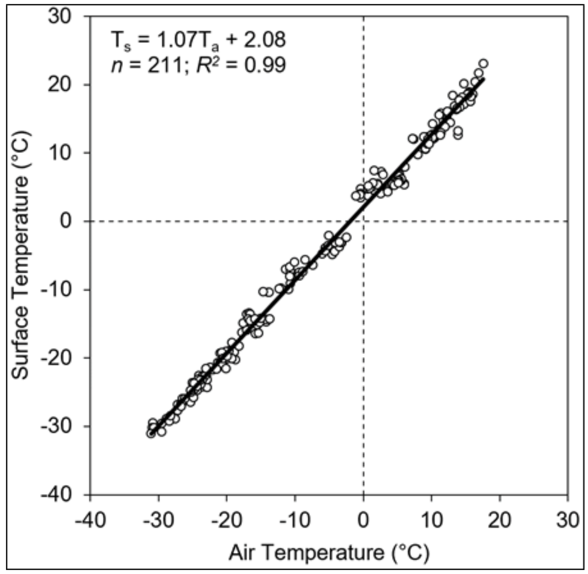

Figure 2. Monthly mean Ta and Ts for the road with the principal axis, 2020–2022.

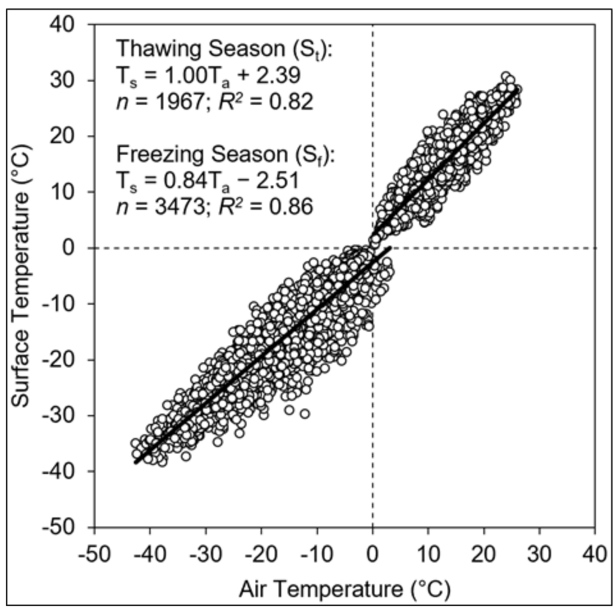

Figure 3. Daily mean Ta and Ts for the road with the principal axis for the freezing and thawing seasons, 2020–2022.

At all sites, FDD totals accumulated analogously throughout most of winter, but at the beginning of the season FDD_a was greater than FDD_s, resulting in low n_f. As the relative increase in FDD_s approached FDD_a, daily cumulative n_f rose and eventually became constant. At the end of the season, the rate of growth slowed and FDD_s departed from FDD_a. In contrast, the relative increase in TDD_s was greater than TDD_a at the beginning of the season likely due to high incident radiation in June, causing high n_t. As the relative increase in TDD_a approached TDD_s, daily cumulative n_t declined and eventually stabilized. Once stabilized the relative increases in degree-day totals for both seasons was about 2–6% per day.

The small range in n-factors indicate the minimal effects of latitude and elevation along the corridor (Table 1). Several studies suggest n-factor variability may be associated with turbulent heat transfer. For example, greater wind speed may decrease n_t and increase n_f (e.g., Sanger 1966).

However, mean annual wind speeds along the corridor were relatively uniform (2–4 m s^{-1}) and vehicle-generated wind effects are unlikely due to the low volume of traffic. Shading from adjacent vegetation could reduce n_t but this is unlikely due to stunted forest growth, brushing in the right-of-way, and high solar elevation in the Arctic. Surfacing materials are relatively uniform along the corridor, but minor differences may cause n-factor variability. For example, lighter surfaces may increase albedo and reduce n-factors. Daily n-factors may vary with the frequency of ploughing in winter and water infiltration from precipitation or dust suppression activities in summer.

Several studies have estimated n-factors for the Dempster–ITH corridor from the available literature. Piamsalee (2019) selected an n_f of 0.80 and an n_t of 1.30 and de Guzman et al. (2021) selected an n_f of 0.95 and an n_t of 1.00. Some of the published values underestimated the measured n-factors presented here. A more conservative embankment design favours overestimated n-factors that assume a thicker active layer and warmer permafrost.

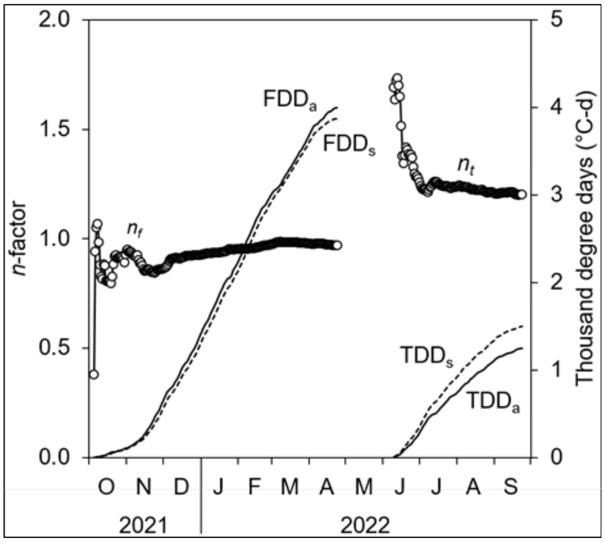

Figure 4. Daily cumulative n-factors and degree days for the air and road at Noell Lake, 2021–2022.

Table 1. Climate and road surface data for the Dempster–ITH corridor over two years beginning in October 2020. Annual mean and seasonal mean temperatures (°C) for the air (T_a) and road surface (T_s), seasonal degree days for the air (FDD_a, TDD_a) and road surface (FDD_s, TDD_s), and mean daily freezing (n_f) and thawing (n_t) n-factors. T_a at Midway Airstrip were used to calculate n-factors at Stony Creek.

	Annual		Freezing Season					Thawing Season				
2020–2021	T_a	T_s	T_a	FDD_a	T_s	FDD_s	n_f	T_a	TDD_a	T_s	TDD_s	n_t
Territorial Border	-6.8	-5.6	-19.1	3682	-19.5	3612	1.06	10.5	1212	12.8	1566	1.29
Stony Creek	-	-5.1	-	-	-19.0	3479	1.01	-	-	13.4	1626	1.23
Midway Airstrip	-6.6	-5.5	-19.6	3723	-19.5	3588	1.00	11.4	1332	13.3	1593	1.21
Peel Plateau	-5.6	-4.5	-18.8	3522	-18.8	3430	1.01	12.4	1496	14.5	1792	1.22
Fort McPherson	-6.7	-4.1	-21.9	4084	-20.6	3781	0.93	13.6	1633	17.9	2269	1.35
Inuvik	-6.8	-5.1	-21.1	4010	-21.5	3894	1.03	12.5	1536	15.6	2027	1.28
Noell Lake	-7.4	-5.7	-21.7	4143	-20.8	3861	0.96	12.1	1426	14.7	1790	1.25
Trail Valley Creek	-8.0	-6.2	-21.7	4209	-21.2	3975	0.98	11.0	1308	13.9	1708	1.33
Husky Lakes	-8.3	-6.6	-22.0	4286	-21.2	3990	0.96	10.5	1256	12.7	1594	1.26
2021–2022												
Territorial Border	-7.0	-5.4	-17.6	3792	-16.9	3571	0.94	10.8	1228	13.0	1584	1.24
Stony Creek	-	-4.6	-	-	-15.7	3288	0.89	-	-	13.6	1616	1.10
Midway Airstrip	-6.0	-5.4	-17.0	3699	-16.6	3545	0.92	13.2	1496	13.6	1583	1.08
Peel Plateau	-5.7	-4.1	-16.7	3543	-16.0	3320	0.89	12.3	1467	14.8	1811	1.29
Fort McPherson	-6.7	-4.4	-19.9	4019	-18.6	3730	0.90	13.0	1592	16.7	2144	1.34
Inuvik	-7.0	-5.6	-19.5	3992	-19.1	3781	0.97	12.0	1444	13.8	1755	1.26
Noell Lake	-7.4	-5.9	-20.0	4063	-19.4	3877	0.95	11.7	1360	14.0	1740	1.28
Trail Valley Creek	-8.0	-6.2	-20.2	4137	-19.3	3877	0.93	10.6	1223	13.3	1629	1.34
Husky Lakes	-8.2	-6.4	-20.7	4193	-19.7	3919	0.94	10.3	1202	12.6	1598	1.33

6.2 Gravel Pit *n*-factors

Values for n_f and n_t at the gravel pits ranged from 0.10–0.76 and 1.00–1.30, respectively (Table 2). At all sites *n*-factors were less than the adjacent road, indicating warmer winter and cooler summer surfaces. Figure 5 is a scatter plot of monthly mean temperatures for T_a and T_s at the pits over two years. During S_t, there is a linear correlation similar to the road between T_a and T_s, but during S_f the data are scattered due to differences in winter surface conditions

The principal axis for S_t indicates the gravel pit surfaces are warmer than the air in summer and about 1.4 °C lower than the adjacent road (Figures 2 and 5). However, at Husky Lakes (Pit 177) in 2021 and Stony Creek in 2022, n_t is at unity because T_s was higher than T_a for about half of S_t. At the other sites, n_t is higher because T_s was higher than T_a for 57–89% of S_t.

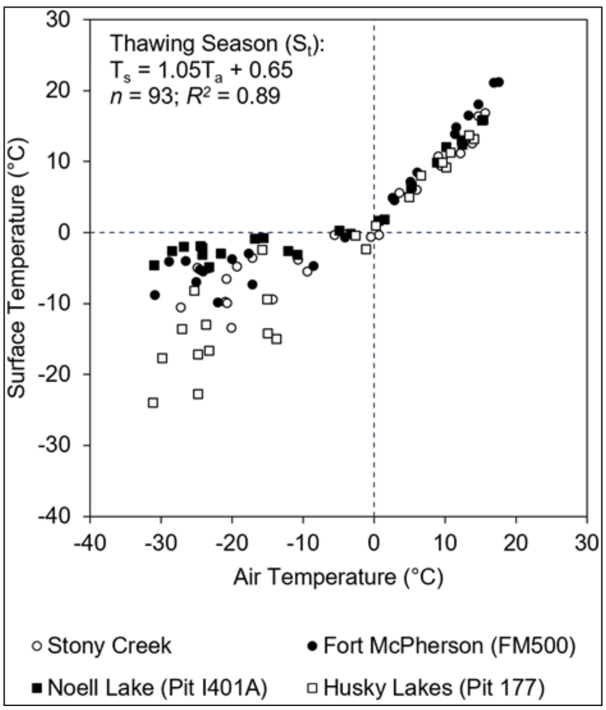

Figure 5. Monthly Ta and Ts at the gravel pits, 2020–2022. The principal axis for the thawing season (St) is given.

At all sites n_f was lower and more variable than the road. Since n_f for the road was relatively consistent, variability at the pits was likely controlled by snow and subsurface thermal conditions. The rank order of n_f was the same in both years but values at all sites were lower in 2021–2022 than in 2020–2021 because snow depth increased.

In the pits, mean n_f was highest at Husky Lakes (Pit 177) where thin snow cover promoted ground surface cooling. Stabilization of n_f occurred about 140 days after n_f at the road. Snow conditions at Stony Creek were associated with strong winds and proximity to the road. Compaction and the introduction of gravel and ice from ploughing increased snow thermal conductivity. Thus, n_f was higher than at sites with lower snow depths (Table 2). Stabilization of n_f occurred in mid winter, about 70 days after n_f at the road.

In both years, n_f were distinct at Fort McPherson (FM500) and Noell Lake (Pit I401A) even though snow depths and T_a were similar (Table 2). T_s was lower at Fort McPherson (FM500) despite having a more insulative snow cover (Figure 6a). These data indicate subsurface conditions influenced winter surface temperatures, and, in turn, n_f. At Noell Lake (Pit I401A), the top of permafrost is at 3.75 m depth with a mean annual temperature (T_p) near 0 °C. In 2021–2022, frost penetration began in early October and active layer freezeback was complete after six weeks (Figure 6b). Although, subsurface ground temperature data are not available at Fort McPherson (FM500), the rapid decline in Ts in mid November indicates a similar freezeback period (Figure 6a).

Table 2. Late winter snow depths (cm) and densities (kg m^3), and mean daily freezing (nf) and thawing (nt) n-factors at the gravel pits over two years beginning in October 2020.

2020–2021	Snow Depth	Snow Density	n_f	n_t
Stony Creek	77.0	500.7	0.54	1.10
Fort McPherson (FM500)	37.0	154.5	0.35	1.26
Noell Lake (Pit I401A)	34.5	224.6	0.13	1.13
Husky Lakes (Pit 177)	8.5	284.6	0.76	1.00
2021–2022				
Stony Creek	147.0	456.7	0.22	1.00
Fort McPherson (FM500)	58.0	115.9	0.19	1.30
Noell Lake (Pit I401A)	58.5	255.6	0.10	1.19
Husky Lakes (Pit 177)	13.5	294.0	0.52	1.15

At Noell Lake (Pit I401A), ground temperatures in the active layer were about -0.3°C throughout S_f (Figure 6b). The thick active layer underlain by permafrost with T_p steadily increasing by 0.5°C during 2017–2022 indicates permafrost at this site is degrading. Water in the active layer, some likely released from permafrost, alters the thermal properties and introduces latent heat effects which prevent rapid ground cooling (Riseborough 1990; Romanovsky and Osterkamp 2000). Thus, n_f is low at sites with thick active layers and warm permafrost because of the continuing release of latent heat during freezing, as evident in the temperatures at 2 m (Figure 6b).

At the Fort McPherson pit (FM500), divergence of TDD_a and TDD_s resulted in high n_t comparable to the road. At the other pits, n_t was closer to one because the relative increase in TDD totals were similar. Field observations showed surface conditions at Fort McPherson (FM500) were relatively dry. Therefore, we suggest lower n_t at the other pits, was associated with the availability of moisture for evaporation, hence similar T_a and T_s.

At the Noell Lake road site, active layer depth was at most 3.25 m and T_p was -4.5°C. Snow clearing as well as low soil moisture and T_p facilitated a shorter freeze back period (four weeks) than at the pit, allowing T_s to decline and n_f to stabilize (Figures 4 and 6c). During S_f, the temperature gradient from the ground surface to the top of permafrost is positive at both sites. The steeper gradient at the road (7.6 °C m^{-1}) increased the heat flux out of the ground, while the low gradient at the pit (1.4 °C m^{-1}) reduced ground cooling (Kokelj et al. 2014).

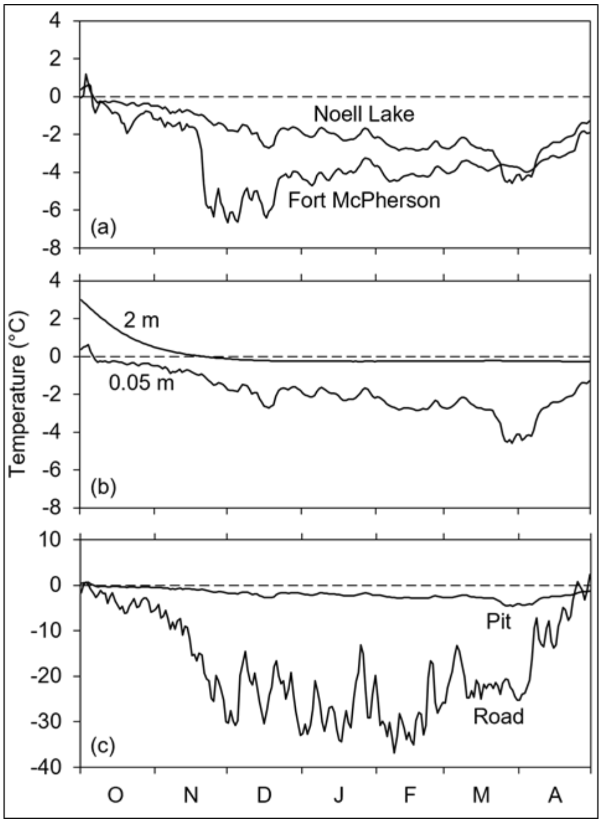

Figure 6. Daily mean ground temperatures from October 2021 to April 2022 at (a) the surface at the Noell Lake (I401A) and Fort McPherson (FM500) pits; (b) the surface and 2 m depth at the Noell Lake pit (I401A); and (c) the surface at the pit and road at Noell Lake.

In 2021–2022, both pits had a similar increase in snow depth but the change in n_f was greater at Fort McPherson (FM500; Table 2). Between years, T_a during S_f increased by about 2 °C at both pits, while T_s increased by 1.0 °C at Noell Lake (Pit I401A) and 3.7 °C at Fort McPherson (FM500). Although increased snow density at Noell Lake (Pit I401A) likely constrained the thermal effects of the deeper snow cover, T_s was less sensitive to changes at the surface because of latent heat effects at depth. These results indicate that surface conditions have less influence on n_f than subsurface conditions where the active layer is deep and permafrost is degrading. Thus, determining *n*-factors for constructed surfaces beneath a homogenous snowpack is complicated by the thermal state of permafrost.

Borrow sources account for a proportion of the thermal disturbance associated with highway construction. These data show surface boundary modifications caused by pit development can lead to permafrost degradation in subarctic settings. Reclamation procedures to preserve permafrost after excavation include natural revegetation, recontouring for drainage, and replacement of the organic layer. At sites with degrading permafrost, additional measures, such as snow compaction, could lower ground temperatures and stabilize thermal conditions. However, these interventions are often difficult to apply in practice. Gravel is a valuable commodity in the Mackenzie Delta region and gravel pits are commonly opened as part of development projects. The effects of permafrost thaw in such pits should be recognized during planning and regulatory review, particularly under a warming climate.

7 CONCLUSIONS

The principal conclusions derived from this study are:

(1) The *n*-factors used to summarize relationships between air and road surface temperatures were relatively consistent along the Dempster–ITH corridor, ranging from 0.89–1.06 for the freezing *n*-factor and 1.08–1.36 for the thawing *n*-factor, with little variation over two years. Values of 0.96 and 1.26 for the freezing and thawing *n*-factors, respectively, appear robust for a gravel road across a range of climatic environments;

(2) At the pits, *n*-factors were less than the road indicating warmer winter and cooler summer surfaces. Snow characteristics had less influence on freezing *n*-factors than ground thermal properties where the active layer is deep and permafrost is degrading; and

(3) Gravel pits experiencing permafrost degradation, such as Noell Lake, would require active mitigation to lower ground temperatures and stabilize thermal conditions. However, permafrost thaw induced by pit development is likely inevitable under a warming climate.

8 ACKNOWLEDGEMENTS

This research was supported by the Natural Sciences and Engineering Research Council of Canada, the Northwest Territories Geological Survey, Aurora Research Institute, and Carleton University. We extend particular thanks to Joel McAlister, Edwin Amos, Ryan McLeod, Greg Elias, Jennifer Humphries, Celtie Ferguson, Eli Nasogaluak, Kathryn Barr, Bill Conley, Miles Dillon, Mary Cockney, Wayne Thrasher, Andrew Koe, Ashley Rudy, and Tim Ensom. Discussions with GNWT-INF and the Imaryuk Monitoring Program improved the study. We thank Richard Blake for sharing embankment data along the corridor, and two anonymous reviewers for their helpful comments.

9 REFERENCES

Alfaro, M.C., Ciro, F.G., Thiessen, K.J., and Ng, T. 2009. ‘Case Study of Degrading Permafrost Beneath a Road Embankment’, *Journal of Cold Regions Engineering* 23(3), pp. 93–111. doi:10.1061/ASCE0887-381X200923:393.

Burn, C.R. 1997. ‘Cryostratigraphy, Paleogeography, and Climate Change During the Early Holocene Warm Interval, Western Arctic Coast, Canada’, *Canadian Journal of Earth Sciences* 34(7), pp. 912–925. doi:10.1139/e17-076.

Burn, C.R. and Kokelj, S.V. 2009. 'The Environment and Permafrost of the Mackenzie Delta Area', *Permafrost and Periglacial Processes* 20(2), pp. 83–105. doi:10.1002/ppp.655.

de Guzman, E.M.B., Alfaro, M.C., Arenson, L.U. and Doré, G. 2021. 'Thermal Regime of Highway Embankments in the Arctic: Field Observations and Numerical Simulations', *Journal of Geotechnical and Geo-environmental Engineering* 147(6), pp. 1–25. doi:10.1061/(ASCE)GT.1943-5606.0002502.

Grozic, E.M. and Zhang, G. 2018. 'Inuvik to Tuktoyaktuk Highway Road Embankment Constructed on Ice-rich Permafrost Terrain', in *GeoEdmonton 2018*, 71st Canadian Geotechnical Conference and 13th Joint CGS/IAH-CNC Groundwater Conference. Edmonton, Alberta, Canada: September 23–26, Paper 256.

Ensom, T., Kokelj, S.V., Morse, P.D., and Kamo McHugh, K. 2020. 'Permafrost Ground Temperature Data Synthesis: 2013-2019 Inuvik–Tuktoyaktuk Highway Region, Northwest Territories', *Northwest Territories Geological Survey* NWT Open Report 2019-020, 13 p.

Environment Canada 2023. *Canadian Climate Normals 1981–2010 Station Data*. Available at: https://climate.weather.gc.ca/climate_normals/index_e.html (Accessed: 7 August 2023).

Huculak, N.A., Twach, J.W., Thomson, R.S., and Cook, R.D. 1978. 'Development of the Dempster Highway North of the Arctic Circle', in *3rd International Conference on Permafrost*. Edmonton, Alberta, Canada: July 10–13, 1978, vol. 1, pp. 798–805.

Instanes, A. and Anisimov, O. 2008. 'Climate Change and Arctic Infrastructure', in *9th International Conference on Permafrost*. Fairbanks, Alaska, United States: Institute of Northern Engineering, University of Alaska Fairbanks, vol. 1, pp. 779–784.

Johnston, G.H. 1981. *Permafrost: Engineering Design and Construction*. New York, New York, United States: John Wiley & Sons.

Johnston, G.H. 1982. 'Design and Performance of the Inuvik, N.W.T., Airstrip', in *4th Canadian Permafrost Conference*. Calgary, Alberta, Canada: March 2–6, 1981, pp. 577–585.

Kokelj, S.V., Lantz, T.C., Wolfe, S.A., Kanigan, J.C., Morse, P.D., Coutts, R., Molina-Giraldo, N. and Burn, C.R. 2014. 'Distribution and Activity of Ice Wedges Across the Forest-tundra Transition, Western Arctic Canada', *Journal of Geophysical Research (Earth Surface)* 119(9), pp. 2032–2047. doi:10.1002/2014/JF003085.

Kokelj, S.V., Lantz, T.C., Tunniclifee, J., Segal, R. and Lacelle, D. 2017. 'Climate-driven Thaw of Permafrost Preserved Glacial Landscapes, Northwestern Canada', *Geology* 45(4), pp. 371–374. doi:10.1130/G38626.1.

Kokelj, S.A., Beel, C.R., Connon, R.F., Graydon, C.E.D., Kokelj, S.V., and Burn, C.R. 2022. 'Peel Plateau Climate Data, Northwest Territories', *Northwest Territories Geological Survey* NWT Open Report 2022-005, 16 p. doi:10.46887/2022-005.

Lingnau, B. 1985. *Observation of the Design and Performance of the Dempster Highway*. University of Alberta, Department of Civil Engineering, Master's thesis.

Lunardini, V.J. 1978. 'Theory of n-factors and Correlation of Data', in *3rd International Conference on Permafrost*. Edmonton, Alberta, Canada: July 10–13, 1978, vol. 1, pp. 40–46.

Mackay, J.R. 1963. 'The Mackenzie Delta Area, N.W.T.', *Geographical Branch, Mines and Technical Surveys* Memoir 8.

Mark, D.M. and Church, M. 1977. 'On the Misuse of Regression in Earth Science', *Mathematical Geology* 9(1), pp. 63–75.

Natural Resources Canada 2023. *Geospatial Data Extraction*. Available at: https://maps.canada.ca/czs/index-en.html (Accessed: 8 August 2023).

Norris, D.K. 1984. 'Geology of the Northern Yukon and Northwestern District of Mackenzie', *Geological Survey of Canada* Map 1581A, scale 1:500000.

O'Neill, H.B., Burn, C.R., Kokelj, S.V. and Lantz, T.C. 2015. ''Warm' Tundra: Atmospheric and Near-surface Ground Temperature Inversions Across an Alpine Treeline in Continuous Permafrost, Western Arctic, Canada', *Permafrost and Periglacial Processes* 26(2), pp. 103–118. doi:10.1002/ppp.1838.

Palmer, M.J., Burn, C.R., and Kokelj, S.V. 2012. 'Factors Influencing Permafrost Temperatures Across Tree Line in the Uplands East of the Mackenzie Delta, 2004–2010', *Canadian Journal of Earth Sciences* 49, pp. 877–894. doi:10.1139/e2012-002.

Piamsalee, A. 2019. *Field and Numerical Studies of an Arctic Highway Embankment Compacted with Frozen Fill over Permafrost*. University of Manitoba, Master's thesis.

Rampton, V.N. 1988. 'Quaternary Geology of the Tuktoyaktuk Coastlands, Northwest Territories', *Geological Survey of Canada* Memoir 423.

Riseborough, D.W. 1990. 'Soil Latent Heat as a Filter of the Climate Signal in Permafrost', in *5th Canadian Permafrost Conference*. Québec City, Québec, Canada: Nordicana, pp. 199–205.

Ritchie, J.C. 1977. 'The Modern and Late Quaternary Vegetation of the Campbell-Dolomite Uplands, near Inuvik, N.W.T., Canada', *Ecological Monographs* 47(4), pp. 401–423.

Romanovsky, V.E. and Osterkamp, T.E. 2000. 'Effects of Unfrozen Water on Heat and Mass Transport Processes in the Active Layer and Permafrost', *Permafrost and Periglacial Processes*, 11(3), pp. 219–239. doi:10.1002/1099-1530(200007/09)11:3<219::AID-PPP352>3.0.CO;2-7.

Rudy, A.C.A., Kokelj, S.V., Morse, P.D., and Ensom, T. 2020a. 'Permafrost Ground Temperature Report: Inuvik to Tuktoyaktuk Highway Sentinel sites, Northwest Territories', *Northwest Territories Geological Survey* NWT Open Report 2019-007, 8 p.

Rudy, A.C.A., Kokelj, S.V., and Ensom, T. 2020b. 'Permafrost Ground Temperature Report: Inuvik to Tuktoyaktuk Highway embankment sites, Northwest Territories', *Northwest Territories Geological Survey* NWT Open Report 2019-016, 8 p.

Sanger, F.J. 1966. 'Degree-days and Heat Conduction in Soils', in *1st International Conference on Permafrost*. Lafayette, Indiana, United States: pp. 253–262.

Thompson, H.A. 1963. 'Freezing and Thawing Indices in Northern Canada', in *1st Canadian Conference on Permafrost*. Ottawa, Ontario, Canada: pp. 18–36.

Wahl, H.E., Fraser, D.B., Harvey, R.C., and Maxwell, J.B. 1987. 'Climate of Yukon', *Environment Canada, Atmospheric Environment Service*, Climatological Studies No. 40.